Defective Chromosome Segregation and Telomere Dysfunction in Aggressive Wilms' Tumors

Ylva Stewénius,[1] Yuesheng Jin,[1] Ingrid Øra,[2,5] Jan de Kraker,[7] Johannes Bras,[6] Attila Frigyesi,[3] Jan Alumets,[4] Bengt Sandstedt,[8] Alan K. Meeker,[9] and David Gisselsson[1]

Abstract

Purpose: In many childhood neoplasms, prognostic subgroups have been defined based on specific chromosome changes. In Wilms' tumor (WT), such subclassification has been hampered by the diverse and relatively unspecific pattern of chromosomal imbalances present in these tumors. Unspecific patterns of cytogenetic imbalances in tumors are often caused by mitotic segregation errors due to short dysfunctional telomeres. As an alternative to cytogenetic classification, we therefore have evaluated whether the rate of telomere-dependent chromosomal instability could influence the clinical course in WT patients.

Experimental Design: Telomere function and mitotic segregation errors were assessed in 12 cultured tumors and in tumor tissue sections from 41 WT patients.

Results: Abnormal telomere shortening was found in cultured cells and in tissue sections from highly aggressive tumors. *In vitro*, dysfunctional telomeres were associated to specific cell division abnormalities, including anaphase bridges and multipolar mitoses. Assessment of mitotic figures in tissue sections revealed that anaphase bridges and multipolar mitoses were predominantly, but not exclusively, present in high-risk tumors and were predictors of poor event-free and overall survival.

Conclusions: Telomere-dependent mitotic instability is present in a subgroup of WT, predominately consisting of high-risk tumors.

Wilms' tumor (WT) is the most common pediatric renal neoplasm, affecting 1 of 10,000 children (1, 2). The overall 5-year survival rate of patients with WT is now 90% (3). One of the remaining challenges in WT management is to find ways to individualize treatment by refining risk stratification. Most WT in Europe are treated preoperatively according to a standardized protocol (4). The postoperative treatment is based on tumor stage and tumor histology found at the time of surgery. Histologically WT is typically composed of a combination of cells derived from different embryonic origins and is classically composed of a combination of epithelial, mesenchymal, and/or blastemal cells (5). Based on histology, preoperatively treated WT can be divided into three prognostic subgroups (4): low-risk tumors, primarily comprising completely necrotic tumors; the intermediate-risk group, comprising tumors of epithelial, stromal, mixed, and regressive type; and tumors with focal anaplasia. The high-risk group includes tumors of blastemal predominant type and tumors with diffuse anaplasia. There have been several attempts to improve the prognostication of WT, e.g., by quantification of telomerase expression (6), global gene expression analysis (7), and cytogenetics. Gain of 1q and loss of 16q and chromosome 22 have been associated with poor outcome (8–10). Loss of heterozygosity for 1q and 16q have also been suggested as adverse prognostic factors (11). Moreover, poor outcome and diffuse anaplasia have been associated with atypical mitoses and aneuploidy/tetraploidy at flow cytometry (4, 12, 13). The criteria for anaplasia include bizarre, often multipolar, mitoses and enlarged hyperchromatic nuclei. In adult tumors, nuclear atypia, pleomorphism, aneuploidy, and mitotic multipolarity have all been connected to an abnormal segregation of chromosomes at cell division (14, 15). Such mitotic instability can result in an elevated mutation rate at the chromosome level, often called chromosomal instability (CIN).

One common cause of CIN in adult tumors is abnormal shortening of telomeric repeat sequences (16). This telomere-dependent CIN leads to loss of protection of chromosome ends. Unprotected chromosome termini may interact with, and attach to, other TTAGGG-deficient termini or broken chromosomes (17). This causes chromosome fusions and dicentric chromosomes that can form bridges at anaphase, which subsequently break and create new reactive chromosome ends.

Authors' Affiliations: Departments of [1]Clinical Genetics, [2]Pediatric Hematology and Oncology, [3]Cardiology, and [4]Pathology, Lund University Hospital, Lund, Sweden; Departments of [5]Human Genetics and [6]Pathology, Academic Medical Center; [7]Department of Pediatric Oncology and Hematology, Emma Kinderziekenhuis, Amsterdam, the Netherlands; [8]Department of Pathology, Karolinska Hospital, Stockholm, Sweden; and [9]Department of Pathology, Division of Genitourinary Pathology, The Johns Hopkins Institutions, Baltimore, Maryland

Received 5/4/07; revised 7/13/07; accepted 9/4/07.

Grant support: Swedish Children's Cancer Foundation, Sharon B. Lund Foundation of American Cancer Society, Lund University Hospital donation funds, Gunnar Nilsson Foundation, and Swärd Foundation.

The costs of publication of this article were defrayed in part by the payment of page charges. This article must therefore be hereby marked *advertisement* in accordance with 18 U.S.C. Section 1734 solely to indicate this fact.

Requests for reprints: Ylva Stewénius, Department of Clinical Genetics, Lund University Hospital, SE-221 85 Lund, Sweden. Phone: 46-46-173398; Fax: 46-46-131061; E-mail: ylva.stewenius@med.lu.se.

©2007 American Association for Cancer Research.

doi:10.1158/1078-0432.CCR-07-1081

Downloaded from clincancerres.aacrjournals.org on October 25, 2020. © 2007 American Association for Cancer Research.

Table 1. Karyotypes of primary tumors and cell lines

Case no.	Age (y)/sex	Histology	Karyotype
1	8/F	I	53,X,-X,+der(1)t(1;10)(p11;q11),+6,+7,+8,+12,+13,+17,+20
2	15/F	H (B)	46,XX,der(16)t(1;16)(q12;q12),t(21;22)(q22;q11)
3	6/F	I	46,XX, der(7)t(7;16)(q31;q23),der(16)t(7;16)(q13;q31)
4	2/F	I	46,XX,t(5;6;16)(q12;q16;q12)/47,idem,+2
5	6/M	I	48,XY,+6,+12,del(18)(q21)
6	4/M	I	48,XY,+12,+13,der(16)t(16;21)(p11;q11),+20,-21/46,XY
7	1/F	H (B)	28,X,+7,+8,+der(9)t(1;9)(q21;q12),+12,+21/56,XX,+7,+7,+8,+8,+der(9)t(1;9)(q21;q12), +der(9)t(1;9)(q21;q12),+12,+12,+21,+21
8	0.8/M	I	46,XX,der(9)t(4;9)(p16;q34)/45,idem,-Y
9	1/F	I	50,XX,+7,+8,+12,+13
10	4/M	I	47,XY,+2/47,XY,+12
11	2/F	H (A)	38-43,XX,der(6)ins(6;5)(q27;?)ins(6;15)(q27;q?)t(6;10)(q27;q11), -8,der(10)t(10;12)(q21;p12), -11,der(12)t(12;13)(q22;q14), der(13)t(11;13)(?p13;q22),tas(15;22)(p13;p13),-16,tas(16;21)(p13;p13), -17, -18,der(19)t(17;19)(q21;q13),-21,-22/67-91<4n>,idemx2,-9,-9
12	<18/F	H (A)	58-68,X,der(X)t(X;11)(p22;q21)x2,der(1)t(1;18)(q21;p11), der(1)t(1;7)(p36;q31),+ins(1;6)(q43;?),+der(2)t(2;8)(q31;p21), der(3)del(10)(q24)ins(3;20)(p11;p10)t(3;10)(p11;q21),-4,+inv(5)(p15q35), +6,del(7)(q22),der(7)t(3;7)(p13;q32)ins(3;9)(p25;?),+der(7)t(4;7)(q25;q32), -8,t(8;8)(p23;q22),-9,der(9)t(9;10)(q23;q24),-10,der(10)del(10)(p11)t(10;21) (q24;q11),del(11)(q23),+der(11)t(11;22)(p15;p11),+12,der(12)t(4;12)(p14;q24), der(12)t(12;18)(q15;p11),+der(12)t(12;18)(q15;p11),-14,-15,del(16)(q13), -17,der(17)t(12;17)(p13,q15)x2,-18,-18,+19,der(19)t(19;21)(p11;q22) t(17;19)(?;q11)t(17;21)(?;q11),der(19)del(19)(p13)t(19)(17;19) (q11;q13),-20,der(20)t(20;20)(p13;q13)t(10;20)(q22;q13),-21,-22

Abbreviations: M, male; F, female; I, intermediate-risk histology; H, high-risk histology; (B), blastemal predominant histology; (A), anaplastic histology.

This breakage-fusion-bridge cycle leads to continuous redistribution of chromosome material in the proliferating tumor cell population (18). Anaphase bridges (AB) may also inhibit the cell division process and result in cells with a duplicated genome, as well as duplicated centrosomes. In the subsequent mitosis, the supernumerary centrosomes may trigger the cells to divide in more than two directions through multipolar mitoses (MM; refs. 19, 20). In WT cells, telomeres are typically shorter than in somatic cells from the same patients (21). Furthermore, telomeric fusions (22) and chromosomal aberrations derived from breakage-fusion-bridge cycles have been described (23). However, the prevalence of telomere-dependent CIN in WT is not known, and it has not been studied whether it has any implications for clonal evolution and the course of disease.

The aim of the present study was to evaluate if CIN was present in WT. We first did *in vitro* studies of 11 primary tumors and one cell line to explore connections between telomere status, mitotic chromosome segregation, and cytogenetic variability in WT. We also attempted to investigate if the rate of chromatid segregation abnormalities *in vivo* correlated to clinical and/or pathologic features by quantifying the rate of chromosome segregation errors in tumor tissue sections.

Materials and Methods

Cultured primary tumors and cell lines. Primary tumor material was obtained from 11 WT biopsies received for cytogenetic analysis (cases 1-11). Seven were from patients treated at University Hospital in Lund, Sweden, and four were from patients treated at Academic Medical Center at Amsterdam, the Netherlands. The cell line WiT 49 (case 12), derived from an anaplastic metastasis to the lung from a pediatric WT, was kindly donated by Dr. Yeger at Laboratory of Medicine and Pathobiology, University of Toronto, Canada (24, 25).

Cell culture and cytogenetic analysis. Cell culture, harvest, and chromosome preparation for banding and fluorescence *in situ* hybridization (FISH) were according to standard methods (26). For analysis of chromosome dynamics at mitosis in tissue cultures, cells were harvested without metaphase arrest and stained with H&E. Anaphase cells and metaphase cells were scored in each case with AB and MM as defined by Jin et al. (27).

FISH analyses of cultured cells. Chromosome-specific centromeric and whole-chromosome painting probes were from Vysis, Inc. Multicolor karyotyping was done by the combined binary and ratio labeling protocol (28). Detection of subtelomeric sequences was done by FISH as described (29). Telomeric TTAGGG repeats were visualized with fluorescein-conjugated $(CCCTAA)_3$ peptide nucleic acid probes (30), and the number of negative chromosome termini was scored in metaphase cells of the lowest ploidy level. At least 10 cells were scored in each case.

Centrosome detection. Cells cultured on chamber slides were briefly washed in PBS, fixated in methanol for 5 min at room temperature, air dried, and incubated for 30 min with rabbit Cy3-labeled monoclonal anti–γ-tubulin and murine FITC-labeled anti–β-tubulin antibodies (Sigma) diluted 1:40 in blocking buffer. At least 100 interphase cells and 50 mitotic cells were analyzed in each case.

Estimation of the rate of copy number change. To estimate the frequency of copy number change in case 12 and in normal fibroblasts, colonies grown from single cells were created by plating single-cell suspension aliquots of 10,000 cells on chamber slides. In case 10, colonies could not be established from single cells. The analysis was therefore done on 20 colonies in a subconfluent chamber slide. This approach may result in overestimation of the rate of copy number change because of cell migration but is not likely to result in an underestimation of this variable. Interphase FISH analysis with probes

Downloaded from clincancerres.aacrjournals.org on October 25, 2020. © 2007 American Association for Cancer Research.

for the centromeres of chromosomes 1 and 7 was done on 20 of the resulting colonies. Chromosomes 1 and 7 were chosen for the analysis, because in case 12 the copy number of chromosome 1 is stable whereas that of chromosome 7 varies among cells. To exclude scoring of polyploidization events, only cells with chromosome copy numbers outside duplicated levels of the stem line copy number were scored as aneuploidy events. The rate of copy number change was calculated as the total number of aneuploidy events divided by the total number of cell divisions.

Analysis of mitotic figures in tissue sections. Material for analysis of mitotic morphology was obtained from a consecutive series of 43 patients presenting with WTs, operated on at Lund University Hospital from 1992 to 2005. Mitotic figures were evaluated in tissue sections stained by H&E. Two cases (one blastemal predominant and one of mixed type) were excluded because of an insufficient number of cell divisions in the nephrectomy specimens. Nephrectomy specimens underwent histopathologic classification by a local pathologist (J.A.) and were also reviewed by an International Society of Pediatric Oncology reference pathologist (B.S.). All but three patients had received preoperative chemotherapy. Risk classification was according to International Society of Pediatric Oncology guidelines (4). At least 100 metaphase and 30 anaphase cells were evaluated in each of the 41 remaining specimens. AB and MM were scored by one observer (D.G.), without prior knowledge of risk classification, stage, or outcome, using the same criteria as for cultured cells. The prognostic effect of mitotic abnormalities for patients was analyzed using Kaplan-Meier analysis with time from diagnosis to any event (local recurrence and/or distant metastases or death of disease) or to last follow up. One patient who

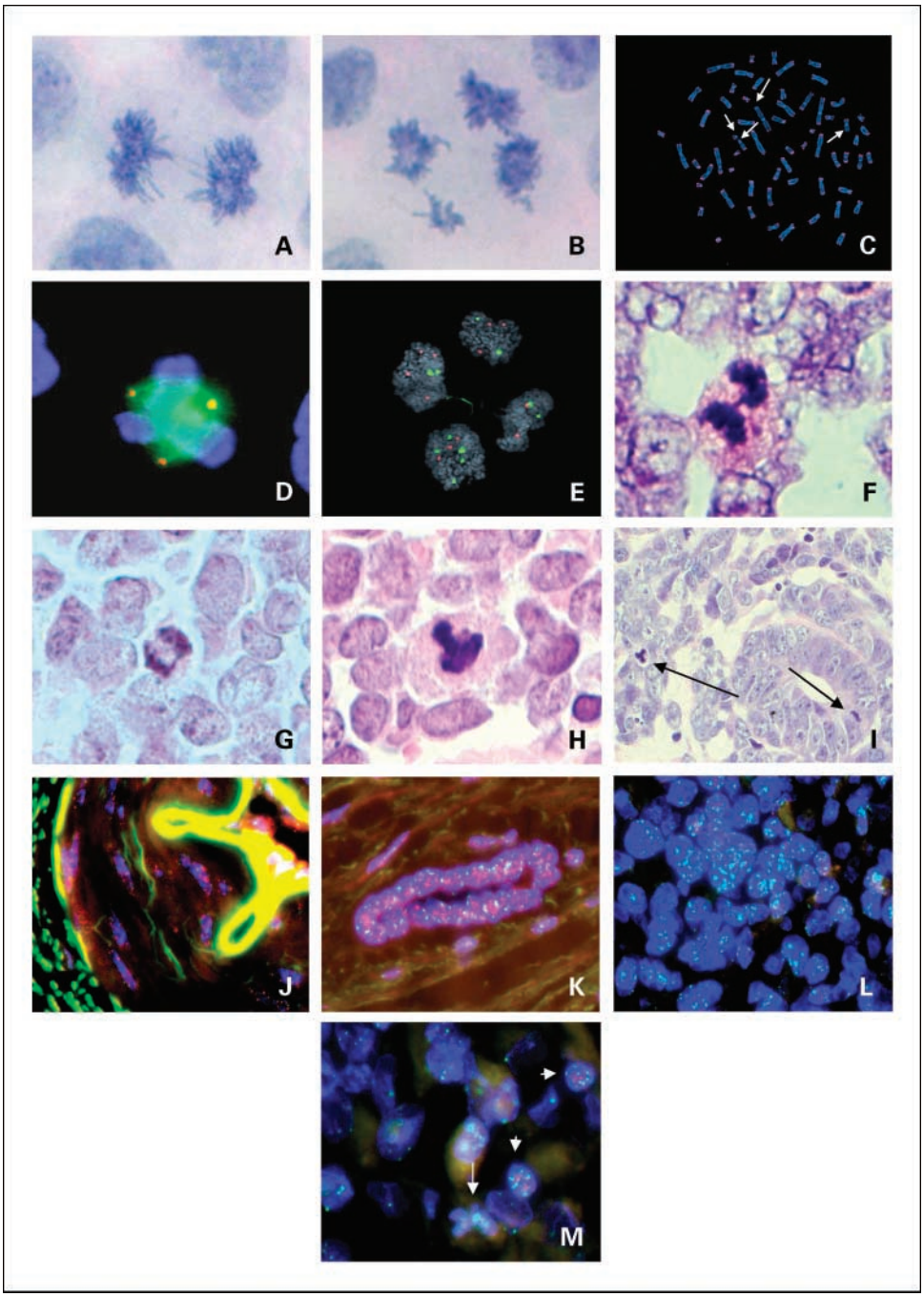

Fig. 1. Telomeric dysfunction and mitotic instability. *A-E,* from case 12. AB involving two chromatids (*A*) and a multipolar anaphase cell (*B*) with four spindle poles stained by H&E. *C,* four TTAGGG-negative chromosome arms in a metaphase cell. *D,* immunofluorescence shows a tripolar metaphase cell organized by three spindle poles (red, centrosomes; green, microtubuli). *E,* chromosome segregation in a multipolar anaphase cell; chromosome 7 (*red centromeric probe*) and chromosome 1 (*green centromeric probe*) segregate in an unbalanced fashion among the daughter cells. ABs in tissue sections from the blastemal components of a mixed type primary WT (case P4; *F*) and a blastemal predominant primary WT (case P5; *G*). *H,* tripolar metaphase cell in the same blastemal predominant tumor (case P5). *I,* multipolar metaphase cell in a blastemal predominant tumor (case P15). Quantitative FISH analysis with telomeric (*J-M*; *red*) and centromeric probes (*K-M*; *green*) and chromatin counterstain (*blue*). *J,* normal intensity telomere signals in the tunica media of a vessel from the tumor capsule (case P16); autofluorescence from elastic fibers in green-yellow. *K,* telomere and centromere signals in a glandular formation (case P11; epithelial tumor component) and in surrounding spindle cells (stromal tumor component), *L,* strong centromere and weak telomere signals in a blastemal component (case P7). *M,* anaplastic component (case P16) with weak telomere signals in pleomorphic cells and an MM (*arrow*); normal signal pattern in monomorphic lymphocyte-like cells (*arrowheads*).

Downloaded from clincancerres.aacrjournals.org on October 25, 2020. © 2007 American Association for Cancer Research.

Table 2. Telomere shortening and mitotic instability

Case	No. TTAGGG-negative chromosome ends*	MMs †	ABs ‡
1	0-1	0/20 (0%)	0/54 (0%)
2	**0-5**	**2/300 (0.6%)**§	**5/35 (14%)**§
3	—‖	0/300 (0%)§	0/30 (0%)§
4	0-1	0/86 (0%)	0/136 (0%)
5	—	0/15 (0%)	0/39 (0%)
6	—	0/19 (0%)	**1/25 (3.8%)**
7	—	0/300 (0%)§	0/30 (0%)§
8	0-1	0/86 (0%)	**3/108 (2.7%)**
9	—	0/103 (0%)	2/115 (1.7%)
10	0-1	0/86 (0%)	0/108 (0%)
11	**>10**¶	**1/72 (1.4%)**	**12/32 (37.5%)**
12	**0-5**	**37/1129 (3.3%)**	**52/697 (7.4%)**

NOTE: Values above cutoff in bold type.
*The range of chromosome arms without signals for telomeric TTAGGG sequences.
† Mitoses scored, percentage of MM in parenthesis.
‡ Anaphase cells scored, percentage of AB in parenthesis.
§Scored in histopathology sections because the amount of tumor material available for culture was limited.
‖Not determined.
¶The exact number was not possible to estimate but the chromosome arms without telomeric signal were in no cell fewer than 10.

died from complications was excluded from event analyses. To test for significant covariates, Wald's test was used. Regional ethics committees at Lund University and Academic Medical Center approved the study.

FISH on tissue sections. Quantitative FISH was done on tissue sections from archival material as described (31) using PNA probes for telomeric TTAGGG sequences and centromeric α satellite sequences (Applied Biosystems). The telomere fluorescence intensity (TFI) was calculated as (total Cy3 intensity)/(total 4′,6-diamidino-2-phenylindole intensity) for each sampled nucleus or population of nuclei. Endothelial nuclei showed consistent TFIs of 0.02 to 0.04 in different tissue sections, and these cells were therefore used as an internal reference to obtain normalized TFIs for individual tumor tissue elements. Typically 50 to 100 nuclei were analyzed for each tissue component.

Results

Cytogenetic abnormalities. Eleven primary WT (cases 1-11) and one established WT cell line (case 12) were characterized by G banding, combined binary and ratio labeling, and subtelomeric FISH (Table 1). Of the primary tumors, eight exhibited intermediate-risk histology and three had high-risk histology: cases 2 and 7 were of blastemal predominant histology and case 11 was diffusely anaplastic. All but case 11 exhibited moderately complex karyotypes. Case 11 exhibited a very complex karyotype with numerous numerical and structural aberrations, including frequent telomere associations that varied among the cells. Case 12 was a cell line derived from a pulmonary metastasis with anaplastic histology. It showed a near-triploid, complex karyotype. Both cases 11 and 12 exhibited extensive intercellular cytogenetic heterogeneity, making it difficult to define individual clones. Thus, in our small subset of cultured tumors, the highly complex karyotypes were limited to the two anaplastic tumors, whereas the remaining cases showed moderately complex or simple karyotypes.

Status of telomeric repeat sequences and gross mitotic abnormalities. To evaluate telomere status and chromosomal segregation abnormalities, H&E staining was used to visualize chromosomes in mitotic figures, and hybridization with telomere-specific probes was done. The mitotic segregation analysis detected two main types of cell division abnormalities in the cultured cells, i.e., AB (Fig. 1A) and MM (Fig. 1B). Five tumors had an elevated rate of AB (Table 2). Three of these tumors (cases 2, 11, and 12) were histopathologically classified as high-risk tumors, and these exhibited higher rates than the others. The remaining high-risk tumor (case 7) did not show an elevated AB rate. The three high-risk tumors that displayed an elevated AB rate also displayed MM. In the remaining two tumors with an elevated AB rate, no MM was detected. The remaining cases showed neither AB nor MM. In normal fibroblasts, the rate of AB was <2% and there were no MM.

Several studies have shown that disrupted telomere protection can contribute to the generation of chromosomal aberrations by disturbances of normal chromosome segregation (17, 18). It has been shown that the number of chromosome arms with TTAGGG-repeat probe signals by FISH correlates well to the protective capacity of telomeres in a cell (26). Metaphase cells for evaluation of telomere status by probes for the telomeric repeat sequences were available from 7 of the 12 cases (Table 2; Fig. 1C). Three of these cases had elevated numbers of chromosome ends lacking telomeric signals. In karyotypically normal fibroblasts used as controls, loss of no more than one telomeric probe signal was observed per cell. The three tumors without telomeric signals at >1 chromosome arm were the same high-risk tumors that displayed the highest rates of AB and exhibited MM. In cases 2 and 12, one to five chromosome arms lacked signals. Case 11 displayed very weak telomere signals, making them difficult to score exactly.

Mitotic multipolarity, supernumerary centrosomes, and cytogenetic heterogeneity. Telomere-dependent AB have been shown to result in unbalanced translocations and whole-chromosome loss (20). In contrast, the consequences of mitotic multipolarity have been little explored. Case 12 contained a high frequency of MM and was therefore selected for further studies of chromosome segregation in this type of cell division. To confirm spindle multipolarity in this case, centrosomes and

Downloaded from clincancerres.aacrjournals.org on October 25, 2020. © 2007 American Association for Cancer Research.

spindle microtubules were detected by immunofluorescence against γ-tubulin and β-tubulin, respectively. Case 12 exhibited multiple (>2) centrosomes in ~4% of interphase cells. All MMs in this case showed supernumerary centrosomes (Fig. 1D). In case 10, which was used as a control and having no MM, supernumerary centrosomes were not found in any cell. To study the segregation of specific chromosomes in MM, centromeric probes for chromosomes 1 and 7 were cohybridized to anaphase cells in case 12 (Fig. 1E). These chromosomes were chosen because, in case 12, the copy number of chromosome 1

Table 3. Clinical data and cell division abnormalities scored in tissue sections

Case	Age (y)/sex	Tumor diameter (cm)	Histology	Stage	Time to relapse (mo)	Sample topography	Follow-up time (y)	Status at last follow-up	AB (%)	MM (%)
P1	3/M	5	I	II	—	Nephrectomy	10	NED	0	0
P2	6/F	12	I	III	—	Nephrectomy	9	NED	0	0
P3	0.4/F	9	I	I		Nephrectomy	8	NED	0	0
					3	Lung			—*	—*
P4	2/M	15	I	II		Nephrectomy	1.5	DOD	4	1
					3	Regional			6	1
					9	Regional			10	1
P5	15/F	10	H (B)	II		Nephrectomy	1	DOD	14	1
					12	Lung			9	2
P6	6/F	12	I	I		Nephrectomy	1.5	DOD	0	0
					12	Regional			-	-
					21	Regional			0	0
					30	Regional			3	0
P7	6/M	13	H (B)	IV		Nephrectomy	1	DOD	11	10
					5	Lung, bone			—	—
P8	6/M	7	I	II	—	Nephrectomy	5.5	NED	0	0
P9	4/F	11	I	I	—	Nephrectomy	4	NED	0	0
P10	4/F	4	I	II	—	Nephrectomy	2	NED	0	0
P11	2/F	10	I	I	—	Nephrectomy	1.5	NED	3	1
P12	6/M	14	I	II	—	Nephrectomy	0.75	NED	0	0
P13	4/M	7	I	II	—	Nephrectomy	1.5	NED	0	0
P14	1/F	12	H (B)	I	—	Nephrectomy	0.5	NED	0	0
P15	4/M	15	H (B)	V		Nephrectomy	1	DOD	8	1
					4	Lung			11	4
P16	0.6/M	15	H (A)	III		Nephrectomy	0.5	DOD	8	2
					4	Regional, lung, brain			—	—
P17	2/M	9	I	I		Nephrectomy	1.5	NED	0	0
P18	4/M	7	I	II		Nephrectomy	2.5	NED	0	0
					8	Regional, lung			0	0
P19	4/M	8	I	III		Nephrectomy	10	NED	0	0
P20	2/F	2	I	I		Nephrectomy	8	NED	0	0
P21	2/F	7; 3	I	V		Nephrectomy	9	NED	0	0
P22	3/M	7	I	IV		Nephrectomy	9	NED	0	0
P23	1/F	8	I	I	6	Nephrectomy	9	NED	0	0
						Contralateral kidney			0	0
P24	1/F	12; 4	I	V		Nephrectomy	8.5	NED	0	0
P25	6/M	12	H (A)	III		Nephrectomy	8	DOC	10	5
P26	7/F	10	I	II		Nephrectomy	8	NED	0	0
P27	18/F	5	H (B)	IV		Nephrectomy	0.1	DOD	3	1
P28	2/M	5	I	IV		Nephrectomy	10	NED	0	0
P29	10/M	14	I	II		Nephrectomy	10	NED	0	0
P30	1/M	4	I	I		Nephrectomy	10	NED	0	0
					84	Contralateral kidney			—	—
P31	8/M	7	I	I		Nephrectomy	10	NED	0	0
P32	9/M	5	I	III		Nephrectomy	9	NED	0	0
P33	4/F	8	I	II		Nephrectomy	12	NED	0	0
P34	3/F	13	I	I		Nephrectomy	13.5	NED	0	0
P35	3/F	4	I	I		Nephrectomy	5	NED	0	0
P36	2/F	14	I	I		Nephrectomy	13	NED	0	0
P37	1/M	11	I	I		Nephrectomy	14	NED	0	0
P38	3/F	11	I	II		Nephrectomy	12	NED	0	0
P39	2/F	9	I	I		Nephrectomy	11.5	NED	0	0
P40	1/M	9	I	I		Nephrectomy	10.5	NED	0	0
P41	0.5/M	7	I	I		Nephrectomy	10	NED	0	0

Abbreviations: (A), anaplastic subtype; (B), blastemal subtype; NED, no evidence of disease; DOD, dead of disease; DOC, dead of complications; AB, frequency of anaphase cells with bridges; MM, frequency of multipolar mitotic cells.
*Not determined.

Downloaded from clincancerres.aacrjournals.org on October 25, 2020. © 2007 American Association for Cancer Research.

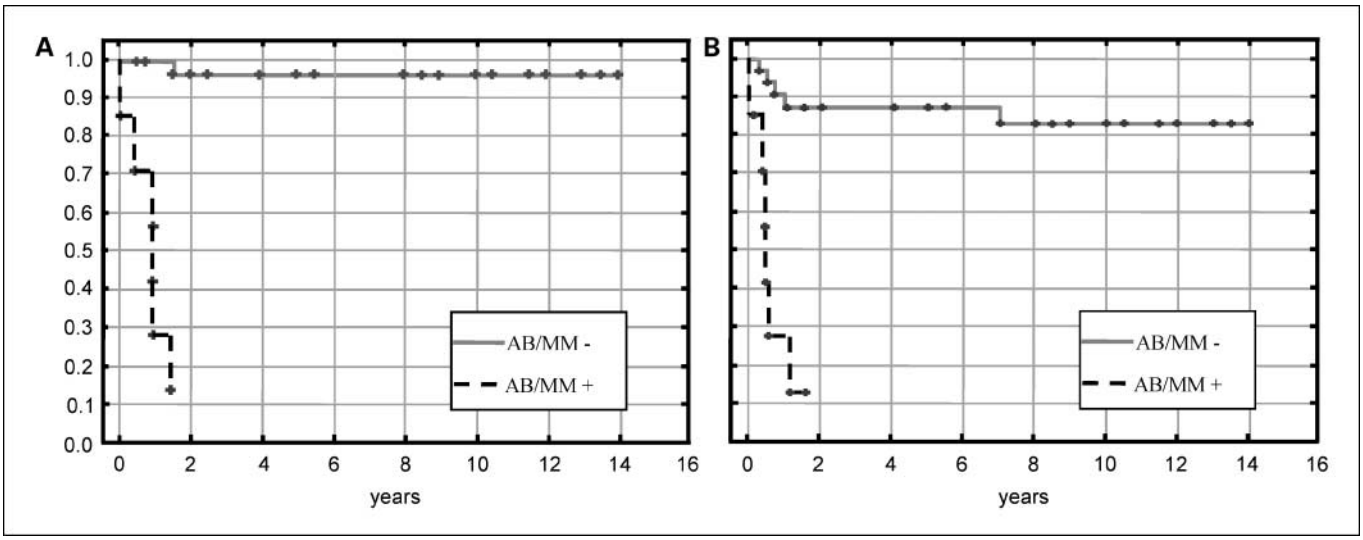

Fig. 2. Kaplan-Meier survival analyses of 41 WT patients. Overall survival (*A*) and event-free survival (*B*). Cases were subdivided according to the presence (AB/MM+) or the absence (AB/MM-) of cell division abnormalities in nephrectomy samples.

was stable whereas that of chromosome 7 varied intercellularly. In bipolar anaphase cells (60; cells with AB not included), these chromosomes segregated in a balanced fashion between the daughter cells. In contrast, in none of the 10 multipolar anaphase cells scored did the daughter cells receive equal numbers of the analyzed chromosomes. In fact, the number of chromosomes in the daughter cells varied between 1 and 7. MM, thus, had the capacity to generate daughter cells with extensive copy number variability.

Mitotic abnormalities and the rate of copy number change. To further investigate the putative connection between copy number heterogeneity and cell division abnormalities, the rate of copy number change was calculated in two WTs: case 10 with a normal telomere status and without mitotic abnormalities and case 12 with extensive telomeric signal loss and a high rate of AB and MM. Monoclonal colonies were analyzed by interphase FISH using centromeric probes for chromosomes 1 and 7, and the rate of copy number change was then calculated from the copy number diversity in these colonies. As a control, 20 monoclonal colonies from fibroblasts were first analyzed. Here, the rate of copy number change for the evaluated chromosomes was approximately one to two per 100 cell divisions (1 of 100 and 2 of 100 for chromosomes 1 and 7, respectively). In case 10, the rate was 1 of 100 cell divisions for both chromosomes and, thus, did not differ from the level in fibroblasts. In case 12, the copy number change was approximately 7 to 10 of 100 cell divisions (10 of 100 and 7 of 100 for chromosomes 1 and 7, respectively). To compare the rates of copy number change thus calculated to the frequency of abnormal mitotic segregation of the same chromosomes, anaphase figures were analyzed with the same centromeric probe system. In normal fibroblasts and in case 10, none of the 100 evaluated anaphase cells showed an abnormal segregation of either chromosome 1 or chromosome 7. In contrast, case 12 exhibited an unbalanced segregation of chromosomes 1 and 7 in several cells, either through anaphase bridging (2 of 118 and 4 of 131 anaphase cells for chromosomes 1 and 7, respectively) or mitotic multipolarity (10 of 118 and 14 of 131 for chromosomes 1 and 7, respectively). The rate of abnormal segregation at anaphase in case 12 (8-11%) thus corresponded very closely to the rate of copy number change calculated from monoclonal colonies (7-10%). This further supports that abnormal mitotic segregation could explain the high rate of copy number change in this case.

Mitotic segregation abnormalities in vivo. To evaluate whether AB and MM were present also in WT cells not subjected to tissue culture, the morphology of dividing cells was analyzed in nephrectomy specimens from 41 patients, as well as biopsies from recurrent tumors and metastases (Table 3). As controls, histologically normal colonic mucosa samples from 20 patients with suspected inflammatory bowel disease were used; here, the frequency of AB was <2% and no multipolar cell divisions were found. Among the WT, eight cases exhibited both AB (Fig. 1F and G) and MM (Fig. 1H), whereas no tumor showed only AB or only MM. In each primary tumor specimen, all viable tissue components were screened for cell division abnormalities. However, AB and MM were only found in anaplastic and blastemal tissue components (Fig. 1I) and not in the epithelial, stromal, or myomatous components. The remaining 33 cases showed no MM and had a frequency of AB below the cutoff level (<2%). Biopsies from recurrent tumors with a sufficient number of cells for cell division analysis were available from only 6 of the 10 patients with recurrent disease. In the three patients with AB and MM in their nephrectomy samples, AB and MM were found also in the samples from regional recurrences and/or distant metastases. Among the cases with recurrent disease that did not show MM/AB in their primary tumors, one patient (case P6) exhibited an elevated frequency of AB at her third recurrence, but no MM; the other cases did not show AB/MM in any of the samples from recurrent tumors. There was a trend toward higher AB/MM values in the recurrent than in the primary tumors ($P = 0.03$ for MM and $P = 0.06$ for AB; primary tumors compared with first recurrence; paired two-sided t test).

Mitotic segregation abnormalities and clinical course. Of the eight primary tumors showing AB/MM, six exhibited high-risk

Downloaded from clincancerres.aacrjournals.org on October 25, 2020. © 2007 American Association for Cancer Research.

histology and two had intermediate-risk histology. Metastatic or local recurrences occurred in five of these cases, whereas six of these patients ultimately died of disease and one from disease complications. Conversely, of the 33 cases not showing mitotic disturbances, one patient died of disease. Kaplan-Meier survival analyses, including all patients except the one dead from complications, showed that the presence of MM/AB was significantly associated with poor overall survival, as well as a lower chance of event-free survival (Fig. 2A and B). No subgroups based on stage or histology contained a sufficient number of patients for statistical evaluation. Thus, the presence of AB/MM was a significant predictor of poor outcome and has a close correlation to the current histologic risk classification.

Telomere length analysis of tissue sections. To assess whether the association between telomere shortening and mitotic disturbances found in cultured cells was present also *in vivo*, we measured telomere length in tumor tissue sections. Five tumors were selected for semiquantitative assessment of TTAGGG-repeat length by measurement of the mean TFI in interphase nuclei (Fig. 1J-M). Cases P13 and P14 (Table 3) were classified as mixed type and blastemal predominant WT, respectively, and were negative for AB and MM. In both these cases, the stromal tumor components had TFIs close to those of the endothelial cells used as controls (Fig. 3). In case P14, normal kidney tissue was also analyzed and showed TFI values completely overlapping with the stromal component of the adjacent WT. The epithelial component in case P13 and the blastemal component in case P14 showed significantly reduced mean TFIs compared with the endothelial control cells ($P < 0.05$; *t* test). However, TFI ranges in these cell populations were wide and overlapped with other tissue elements. Case 11 was a mixed type WT with focal anaplasia, showing AB and MM in the anaplastic component. Here, quantitative FISH showed a dramatically reduced TFI in anaplastic tumor foci, whereas telomere signals were generally stronger in the other tissue elements ($P < 0.05$; anaplastic compared with all other). Very low TFIs were also observed in the majority of cells in case P16, a diffusely anaplastic tumor with AB and MM, and in the

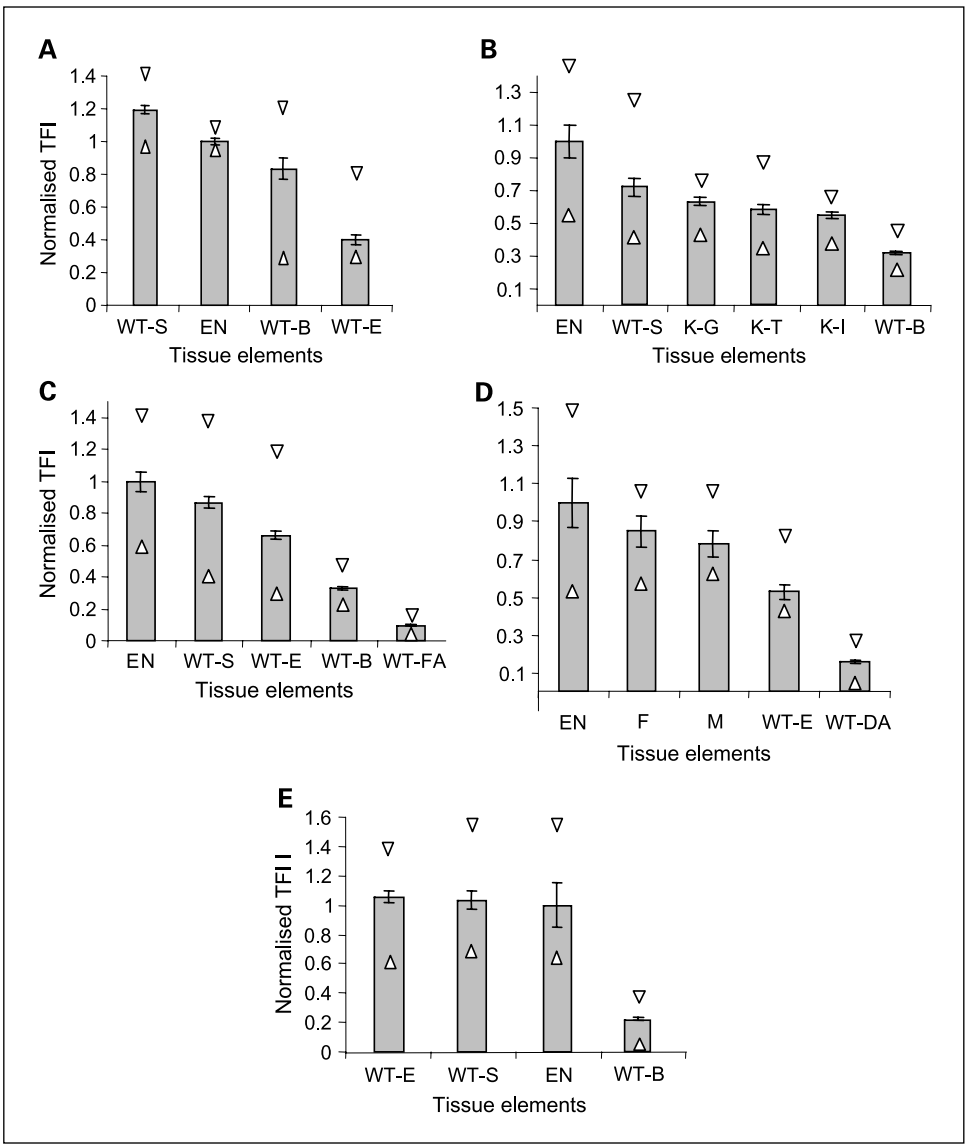

Fig. 3. Mean TFI relative to endothelium. Whiskers, 95% confidence intervals; arrowheads, ranges. The tumor tissue elements analyzed were stromal (*WT-S*), epithelial (*WT-E*), blastemal (*WT-B*), focal anaplastic (*WT-FA*), and diffuse anaplastic (*WT-DA*). Nonneoplastic reference cells were from endothelium (*EN*), kidney glomeruli (*K-G*), kidney tubuli (*K-T*), kidney interstitium (*K-I*), capsule fibroblasts (*F*), and arteriolar tunica media (*M*). *A,* mixed type WT (case P13; Table 4), negative for AB/MM. *B,* blastemal predominant WT (case P14), negative for AB/MM. *C,* mixed type WT (case P11), with AB/MM in focal anaplastic component. *D,* diffusely anaplastic WT (case P16), with AB/MM in anaplastic component. *E,* blastemal predominant WT (case P7) with AB/MM in blastemal component.

Downloaded from clincancerres.aacrjournals.org on October 25, 2020. © 2007 American Association for Cancer Research.

blastemal component of case P7, a blastemal predominant tumor with AB and MM. In none of the AB/MM-positive cases did the TFIs for individual nuclei in the cell population with shortest telomeres overlap with those of the other observed tissue elements. Thus, in contrast to the two AB/MM-negative cases, these tumors seemed to contain distinct cell populations with extremely short telomeres.

Discussion

Abnormal mitotic segregation of chromosomes triggered by dysfunctional telomeres is known to cause an elevated rate of mutations on the chromosome level (CIN) in several adult epithelial and mesenchymal tumor types (16, 26, 32). The aim of the present study was to evaluate whether similar processes are present in WT and whether these phenomena may have any influence on the clinical course. To evaluate the rate of telomere-dependent CIN, it is not sufficient to study only telomere status and chromosomal aberrations. Chromosomal aberrations *per se* do not provide information about their origin, and telomere status alone does not provide any information about its ability to cause CIN. The link between telomere dysfunction and chromosomal aberrations is the formation of functionally dicentric chromosomes that may fail to segregate normally at mitosis because of anaphase bridging. By studying the rate of AB and comparing it to telomere status, it is possible to determine whether telomere-dependent CIN is present in a cell population (33).

In the present study, we found abnormally short telomeres in combination with abnormal mitotic segregation in cultured cells from 3 of 12 WTs. Among the three cases wherein telomere-dependent CIN was found in cultured cells, the highest levels of TTAGGG-negative termini and AB were in the two anaplastic tumors, although it should be taken into consideration that one of these tumors is an established cell line that has been in culture for an extended period of time. Also a blastemal predominant tumor (case 2) displayed telomere dysfunction and an elevated rate of AB. Cultured cells were not available for analysis of mitotic segregation in this case, but elevated AB and MM were observed in archived tumor tissue sections. The fourth high-risk tumor, case 7 of blastemal predominant histology, did not display any mitotic abnormalities or telomere deficiency. Two intermediate-risk tumors displayed a slightly elevated rate of AB; however, neither telomere deficiency nor MM were detected. Thus, our data from cultured WT cells indicated that telomere-dependent chromosome bridging was present in some cases of WT and could be confined to high-risk tumors.

The presence of MM is one of the criteria for the histologic subtype of anaplasia in WT. From studies of MM in other tumors, it is known that MM can be associated to telomere deficiency and anaphase bridging (20) and is typically caused by supernumerary centrosomes (15). Because only relatively few MMs were found in the cultured tumors, no statistical analysis could be made on the association between telomere status and the presence of MM. However, MMs were only found in tumors that displayed telomere loss. Furthermore, all MMs that were analyzed by immunofluorescence in the present study showed two or more centrosomes. The frequencies of AB and MM are positively correlated in many types of neoplasia (20, 34, 35). In the present study, MM was never present in the cultured WT cells or tissue sections without AB being present as well. A possible cause of centrosome duplication could be that AB mechanically inhibits cytokinesis and that the two centrosomes reduplicate before the next mitosis (20, 26, 35). In colorectal cancer cells, it has been shown that the distribution of chromosomes among the spindle poles in MM is close to random (20). The present study shows a similar scenario in WT. FISH with centromeric probes showed that the distribution of individual chromosomes among spindle poles was never equal. Furthermore, detailed analysis of case 12 showed that the rate of copy number change detected in interphase cells during colony growth was highly similar to that predicted from the combined effect of AB and MM. It is thus possible that MM and AB acts in conjunction to generate genetic diversity in growing WT cells and may be dependent on the same mitotic check point deficiencies. MM has indeed been associated with oncogene activation, as well as tumor suppressor gene inactivation. Altered regulation of Aurora kinases (36) and expression of human papilloma virus oncogenes *e6* and *e7* (37) may disturb the integrity of the mitotic machinery independently, as well as through their influence on *TP53* expression. *TP53* is pivotal to cell cycle control, and loss of *TP53* activity may cause supernumerary centrosomes, both through its role in monitoring the genome and allowing polyploid cells to survive and by its direct effect on the centrosome (38). However, it is possible that mitotic multipolarity is merely a symptom of telomere shortening and AB and that it does not generate clonal chromosomal aberrations. In colorectal cancer cell lines, it has been shown that daughter cells from MM have reduced viability, which could imply that the chromosomal aberrations are not passed on to new generations of cells (20). In WT, with karyotypes frequently showing numerical aberrations, MM could be an explanatory model. On the other hand, MM seems to be a rare and possibly a late feature of tumor development, as it is most common in high-risk tumors. It is therefore unlikely that MM is the primary cause of numerical aberrations seen in WT. That also seems to be the case with telomere deficiency and anaphase bridging. It is thus unlikely that telomere-dependent CIN causes the typical intermediate-risk WT karyotype. By analyzing the parental origin of chromosomes in hyperdiploid childhood acute lymphoblastic leukemia (39), it has been shown that the likely origin of the hyperdiploid karyotype is one aberrant mitosis. However, what causes this mitosis is not known. A similar process could underlie numerical changes in WT, although other mechanisms, such as nontelomere-dependent continuous gains and losses of chromosomes are also possible.

AB and MM were observed in nephrectomy tissue sections from 8 of 41 tumors in our material. In the present study, the presence of AB and MM was negatively correlated to overall and disease-free survival. Of the 33 patients with intermediate-risk tumors, one exhibited AB/MM and two died of disease. Among the eight patients with high-risk tumors, one died from complications and six of disease; all of these six cases exhibited AB/MM in the nephrectomy samples. As only 41 tumors were included in this study, the number of cases in the individual subgroups was not sufficient for further statistical analysis. It is therefore not possible to exclude with certainty that MM/AB adds additional information to the current International Society of Pediatric Oncology histologic risk stratification. As the aim of this study was primarily to make a first survey of the

Downloaded from clincancerres.aacrjournals.org on October 25, 2020. © 2007 American Association for Cancer Research.

extent to which telomere dysfunction and CIN were present in WT, we did not include studies of interobserver or intraobserver variability in AB/MM scoring. Finally, the present data do not readily explain why AB and MM are correlated to aggressive disease. A high rate of CIN may give tumor cells the advantage of a faster clonal evolution and progression. An elevated mutation rate might also be of importance for developing therapy resistance and thereby contribute to a worse tumor outcome. *In vitro* model systems have shown that AB may contribute to amplification of genes conferring resistance to chemotherapeutic agents (40). How important this phenomenon is in WT is not known, but one case with amplification and overexpression of the *multidrug resistance–associated protein 1* gene has been observed (41). Genomic amplification in WT has primarily been observed in anaplastic tumors (42), but the underlying mechanisms have not been elucidated.

Five tumors were chosen for further analysis of telomere length in tissue sections; two of the tumors did not exhibit mitotic abnormalities, whereas three did. In all tumors, telomere length differed between histologic regions. However, in the tumors without AB and MM, telomere length overlapped between all histologic regions of the tumors. This was not the case between regions of anaplastic or blastemal histology and other histologic regions in the tumors with AB and MM, and these regions displayed significantly shorter telomeres. This was in accordance with the findings of AB and MM predominately in regions of either anaplastic histology or blastemal histology in the total series of 41 tumors. Thus, telomere deficiency is not only seen in cultured cells and can be ruled out as solely an artifact of cell culturing. It is therefore possible that the histologic features associated with anaplasia (MM, nuclear enlargement, and hyperchromatic nuclei) could be caused by accumulation of chromosome material resulting from cell division failure associated to telomere deficiency and AB (20). As mitotic abnormalities are seen predominately in blastemal and anaplastic regions of tumors and with a higher rate in anaplastic regions, it is possible that there is a development from blastemal to anaplastic histology that is caused by progressive telomere shortening. This further indicates that measurements of telomere length and/or mitotic segregation errors could be helpful to objectively differentiate between blastemal and anaplastic WT elements.

Evidently, further studies of the connection between mitotic instability, on the one hand, and cell biological and clinical features, on the other hand, are warranted in WT.

References

1. Gustafsson G, Langmark F, Heyman M, Wesenberg F, de Verdier B, Arola M. Childhood Cancer in the Nordic Countries. NOPHO Annual Report, Tampere 2006.
2. Pastore G, Znaor A, Spreafico F, Graf N, Pritchard-Jones K, Steliarova-Foucher E. Malignant renal tumours incidence and survival in European children (1978-1997): Report from the Automated Childhood Cancer Information System project. Eur J Cancer 2006;42:2103–14.
3. Tournade MF, Com-Nougue C, de Kraker J, et al. Optimal duration of preoperative therapy in unilateral and nonmetastatic Wilms' tumor in children older than 6 months: results of the Ninth International Society of Pediatric Oncology Wilms' Tumor Trial and Study. J Clin Oncol 2001;19:488–500.
4. Vujanic GM, Sandstedt B, Harms D, Kelsey A, Leuschner I, de Kraker J. Revised International Society of Paediatric Oncology (SIOP) working classification of renal tumors of childhood. Med Pediatr Oncol 2002; 38:79–82.
5. Scott RH, Stiller CA, Walker L, Rahman N. Syndromes and constitutional chromosomal abnormalities associated with Wilms' tumour. J Med Genet 2006;43:705–15.
6. Dome JS, Bockhold CA, Li SM, et al. High telomerase RNA expression level is an adverse prognostic factor for favorable-histology Wilms' tumor. J Clin Oncol 2005;23:9138–45.
7. Zirn B, Hartmann O, Samans B, et al. Expression profiling of Wilms' tumors reveals new candidate genes for different clinical parameters. Int J Cancer 2006; 118:1954–62.
8. Bown N, Cotterill SJ, Roberts P, et al. Cytogenetic abnormalities and clinical outcome in Wilms' tumor: a study by the U.K. cancer cytogenetics group and the U.K. Children's Cancer Study Group. Med Pediatr Oncol 2002;38:11–21.
9. Hing S, Lu YJ, Summersgill B, et al. Gain of 1q is associated with adverse outcome in favorable histology Wilms' tumors. Am J Pathol 2001;158:393–8.
10. Kullendorff CM, Soller M, Wiebe T, Mertens F. Cytogenetic findings and clinical course in a consecutive series of Wilms' tumors. Cancer Genet Cytogenet 2003;140:82–7.
11. Grundy PE, Breslow NE, Li S, et al. Loss of heterozygosity for chromosomes 1p and 16q is an adverse prognostic factor in favorable-histology Wilms' tumor: a report from the National Wilms' Tumor Study Group. J Clin Oncol 2005;23:7312–21.
12. Dome JS, Cotton CA, Perlman EJ, et al. Treatment of anaplastic histology Wilms' tumor: results from the fifth National Wilms' Tumor Study. J Clin Oncol 2006; 24:2352–8.
13. Iyer VK, Kapila K, Agarwala S, Dinda AK, Verma K. Wilms' tumor. Role of fine needle aspiration and DNA ploidy by image analysis in prognostication. Anal Quant Cytol Histol 1999;21:505–11.
14. Gisselsson D, Björk J, Höglund M, et al. Abnormal nuclear shape in solid tumors reflects mitotic instability. Am J Pathol 2001;158:199–206.
15. Saunders WS, Shuster M, Huang X, et al. Chromosomal instability and cytoskeletal defects in oral cancer cells. Proc Natl Acad Sci U S A 2000;97: 303–8.
16. Meeker AK, Argani P. Telomere shortening occurs early during breast tumorigenesis: a cause of chromosome destabilization underlying malignant transformation? J Mammary Gland Biol Neoplasia 2004;9: 285–96.
17. Sabatier L, Ricoul M, Pottier G, Murnane JP. The loss of a single telomere can result in instability of multiple chromosomes in a human tumor cell line. Mol Cancer Res 2005;3:139–50.
18. McClintock B. The stability of broken ends of chromosomes in *Zea mays*. Genetics 1940;26:234–82.
19. Meraldi P, Nigg EA. The centrosome cycle. FEBS Lett 2002;521:9–13.
20. Stewénius Y, Gorunova L, Jonson T, et al. Structural and numerical chromosome changes in colon cancer develop through telomere-mediated anaphase bridges, not through mitotic multipolarity. Proc Natl Acad Sci U S A 2005;102:5541–6.
21. Butler MG, Sciadini M, Hedges LK, Schwartz HS. Chromosome telomere integrity of human solid neoplasms. Cancer Genet Cytogenet 1996;86:50–3.
22. Fett-Conte AC, Liedtke Junior H, Chaves H, Thome JA, Tajara EH. Telomeric fusions in a Wilms' tumor. Cancer Genet Cytogenet 1993;69:141–5.
23. Sawyer JR, Goosen LS, Stine KC, Thomas JR. Telomere fusion as a mechanism for the progressive loss of the short arm of chromosome 11 in an anaplastic Wilms' tumor. Cancer 1994;74:767–73.
24. Alami J, Williams BR, Yeger H. Expression and localization of HGF and met in Wilms' tumours. J Pathol 2002;196:76–84.
25. Alami J, Williams BR, Yeger H. Derivation and characterization of a Wilms' tumour cell line, WiT 49. Int J Cancer 2003;107:365–74.
26. Gisselsson D, Jonson T, Petersén Å, et al. Telomere dysfunction triggers extensive DNA fragmentation and evolution of complex chromosome abnormalities in human malignant tumors. Proc Natl Acad Sci U S A 2001;98:12683–8.
27. Jin Y, Stewénius Y, Lindgren D, et al. Distinct mitotic segregation errors mediate chromosomal instability in aggressive urothelial cancers. Clin Cancer Res 2007; 13:1703–12.
28. Tanke HJ, Wiegant J, van Gijlswijk RP, et al. New strategy for multi-colour fluorescence *in situ* hybridisation: COBRA: combined binary ratio labeling. Eur J Hum Genet 1999;7:2–11.
29. Stewénius Y, Tanke HJ, Wiegant J, Gisselsson D. Cryptic terminal chromosome rearrangements in colorectal carcinoma cell lines detected by subtelomeric FISH analysis. Cytogenet Genome Res 2006;114: 257–62.
30. Lansdorp PM, Verwoerd NP, van de Rijke FM, et al. Heterogeneity in telomere length of human chromosomes. Hum Mol Genet 1996;5:685–91.
31. Meeker AK, Gage WR, Hicks JL, et al. Telomere length assessment in human archival tissues: combined telomere fluorescence *in situ* hybridization and immunostaining. Am J Pathol 2002;160:1259–68.
32. Gisselsson D, Pettersson L, Höglund M, et al. Chromosomal breakage-fusion-bridge events cause genetic intratumor heterogeneity. Proc Natl Acad Sci U S A 2000;97:5357–62.
33. Montgomery E, Wilentz RE, Argani P, et al. Analysis of anaphase figures in routine histologic sections distinguishes chromosomally unstable from chromosomally stable malignancies. Cancer Biol Ther 2003;2: 248–52.

Downloaded from clincancerres.aacrjournals.org on October 25, 2020. © 2007 American Association for Cancer Research.

34. Gisselsson D. Mitotic instability in cancer: is there method in the madness?. Cell Cycle 2005;4:1007–10.
35. Gisselsson D, Jonson T, Yu C, et al. Centrosomal abnormalities, multipolar mitoses, and chromosomal instability in head and neck tumours with dysfunctional telomeres. Br J Cancer 2002;87:202–7.
36. Zhou H, Kuang J, Zhong L, et al. Tumour amplified kinase STK15/BTAK induces centrosome amplification, aneuploidy and transformation. Nat Genet 1998; 20:189–93.
37. Duensing S, Lee LY, Duensing A, et al. The human papillomavirus type 16 E6 and E7 oncoproteins cooperate to induce mitotic defects and genomic instability by uncoupling centrosome duplication from the cell division cycle. Proc Natl Acad Sci U S A 2000;97: 10002–7.
38. Saunders W. Centrosomal amplification and spindle multipolarity in cancer cells. Semin Cancer Biol 2005; 15:25–32.
39. Paulsson K, Mörse H, Fioretos T, Behrendtz M, Strombeck B, Johansson B. Evidence for a single-step mechanism in the origin of hyperdiploid childhood acute lymphoblastic leukemia. Genes Chromosomes Cancer 2005;44:113–22.
40. Coquelle A, Pipiras E, Toledo F, Buttin G, Debatisse M. Expression of fragile sites triggers intrachromosomal mammalian gene amplification and sets boundaries to early amplicons. Cell 1997;89:215–25.
41. Goldstein M, Rennert H, Bar-Shira A, Burstein Y, Yaron Y, Orr-Urtreger A. Combined cytogenetic and array-based comparative genomic hybridization analyses of Wilms' tumors: amplification and overexpression of the multidrug resistance associated protein 1 gene (MRP1) in a metachronous tumor. Cancer Genet Cytogenet 2003;141:120–7.
42. Tretiakova M, Turkyilmaz M, Grushko T, et al. Topoisomerase II α in Wilms' tumors: gene alterations and immunoexpression. J Clin Pathol 2006;59: 1272–7.

Downloaded from clincancerres.aacrjournals.org on October 25, 2020. © 2007 American Association for Cancer Research.

AACR American Association for Cancer Research

Clinical Cancer Research

Defective Chromosome Segregation and Telomere Dysfunction in Aggressive Wilms' Tumors

Ylva Stewénius, Yuesheng Jin, Ingrid Øra, et al.

Clin Cancer Res 2007;13:6593-6602.

Updated version Access the most recent version of this article at:
http://clincancerres.aacrjournals.org/content/13/22/6593

Cited articles This article cites 41 articles, 13 of which you can access for free at:
http://clincancerres.aacrjournals.org/content/13/22/6593.full#ref-list-1

Citing articles This article has been cited by 1 HighWire-hosted articles. Access the articles at:
http://clincancerres.aacrjournals.org/content/13/22/6593.full#related-urls

E-mail alerts Sign up to receive free email-alerts related to this article or journal.

Reprints and Subscriptions To order reprints of this article or to subscribe to the journal, contact the AACR Publications Department at pubs@aacr.org.

Permissions To request permission to re-use all or part of this article, use this link
http://clincancerres.aacrjournals.org/content/13/22/6593.
Click on "Request Permissions" which will take you to the Copyright Clearance Center's (CCC)
Rightslink site.

Downloaded from clincancerres.aacrjournals.org on October 25, 2020. © 2007 American Association for Cancer Research.